Study on the enhancement of flow control authority using DBD plasma actuators

Report Number: R23EACA26
Subject Category: JSS Inter-University Research
URL: https://www.jss.jaxa.jp/en/ar/e2023/23748/

Responsible Representative

Kengo Asada, Postdoctral Researcher, Department of Information and Computer Technology, Faculty of Engineering, Tokyo University of Science

Contact Information

Kengo Asada(asada@rs.tus.ac.jp)

Members

Kengo Asada, Takuto Ogawa

Abstract

The project develops flow control technology by using dielectric barrier discharge (DBD) plasma actuators to establish highly efficient and robust vehicle systems such as rockets, aircraft, and motor vehicles. We aim to enhance the flow control authority of the DBD plasma actuator to adapt unsteady flows over the vehicles through a series of high-fidelity unsteady simulations.

Reasons and benefits of using JAXA Supercomputer System

To perform large-scale three-dimensional unsteady flow simulations using the compressible fluid solver LANS3D, which has a wealth of computational achievements with a JAXA supercomputer system.

Achievements of the Year

This project has conducted high-fidelity flow simulations around the NACA0015 airfoil (Reynolds number 63,000) to establish flow separation control technology using DBD plasma actuators (PA, Fig 1). Through the project, we have proposed and verified the performance of a feedback control model that changes the PA drive method depending on the situation. In addition, in PA burst drive (a drive method that periodically switches ON/OFF), the nondimensional burst frequency F+, considered effective for suppressing flow separation, has conventionally been a value of 1 or 6. On the other hand, relatively high frequencies of 10 or more have been found to be effective at low angles of attack before stall.

Therefore, in FY2023, we conducted high-fidelity simulations to confirm whether the burst drive using such a high frequency effectively controls separation even at high angles of attack where large-scale separation occurs. The PA was installed at 5% of the chord length from the leading edge of the airfoil, and the angle of attack was 14 degrees after the stall angle of attack. In addition to the nondimensional burst frequencies of 1 and 6, which have been considered effective, higher frequencies of 18 and 30 were considered.

Figure 2 shows the time history of L/D during control for each burst frequency. The horizontal axis is the nondimensional time T. Previous studies showed that F+=1 can maintain a high lift to some extent at high angles of attack, but it is impossible to maintain a high L/D due to the increase of drag. In addition, F+=6 can effectively suppress separation at 12 degrees near the stall angle of attack, but as shown in Fig. 2, the F+=6 cannot maintain attached flow at even higher angles of attack, such as 14 degrees. L/D also decreases over time. On the other hand, it can be seen that L/D can be maintained high in the cases using relatively high burst frequencies, especially F+=15, 18, and 20, which were newly simulated this FY. However, higher frequency does not necessarily mean more effective; for example, in the case of F+=30, L/D cannot be improved.

Figure 3 shows the instantaneous flow fields of characteristic cases. The isosurface is the second invariant of the velocity gradient tensor colored by the chordwise directional velocity and represents the vortex structure. In the case of F+=6, separation is suppressed at T=5, and it can be seen that the flow transitions to turbulence and flows along the airfoil surface. However, at T=11, as shown in Fig. 3, flow separation gradually progresses from the airfoil's trailing edge, leading to large-scale separation. On the other hand, in the case of F+=18, the flow is along the airfoil surface even at T=14, and the flow maintains its attached state. To consider the reason for this difference by comparing the flow fields of F+=6 (T=5) and 18 (T=14). At around 10% of the chord length, the flow of F+=6 transitions to turbulent flow with a complex vortex structure, but at F+=18, the vortex structure in the spanwise direction (y-axis direction) induced by PA is maintained up to around 20% of the chord length. These spanwise vortices may play an important role in suppressing separation. However, although the spanwise vortices are observed more clearly in F+=30, the flow separates from the leading edge. These facts indicate that the balance between the maintenance of spanwise vortices and the timing of the turbulent transition is important. We would like to discuss the mechanism in more detail in the future.

As shown above, in FY2020, we conducted a high-fidelity simulation of the NACA0015 airfoil flow at the angle of attack of 14 degrees. The results show that the burst drive at F+=18 effectively suppresses separation, and vortices in the spanwise direction may play an important role in suppressing the flow separation.

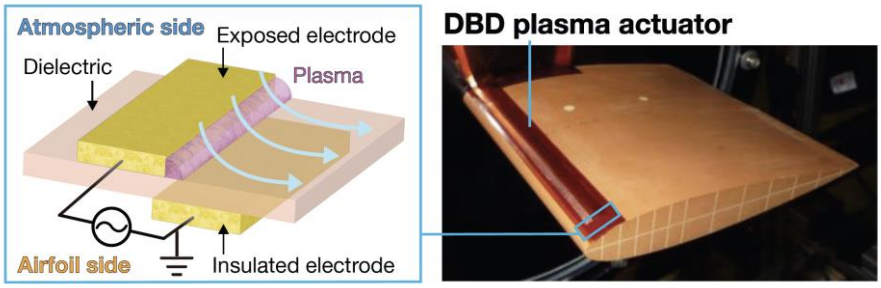

Fig. 1: Schematic of DBD plasma actuator

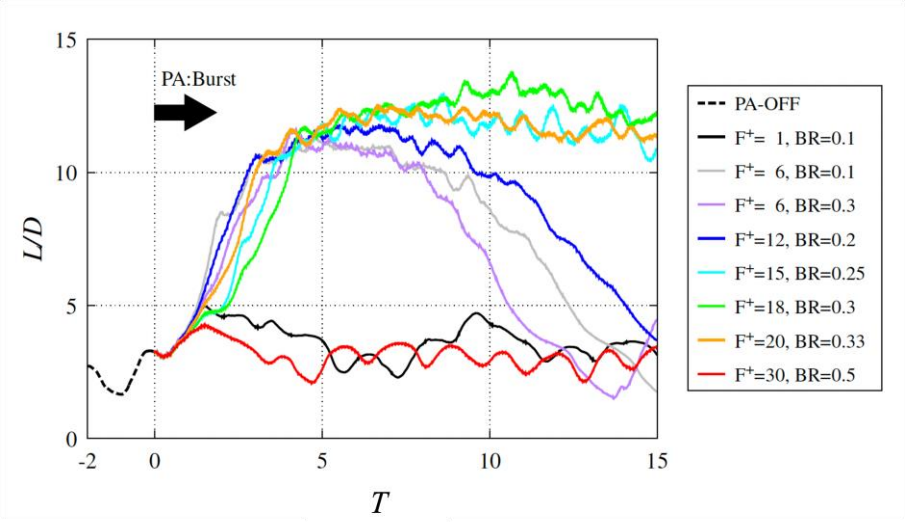

Fig. 2: Time history of the lift-to-drag ratio

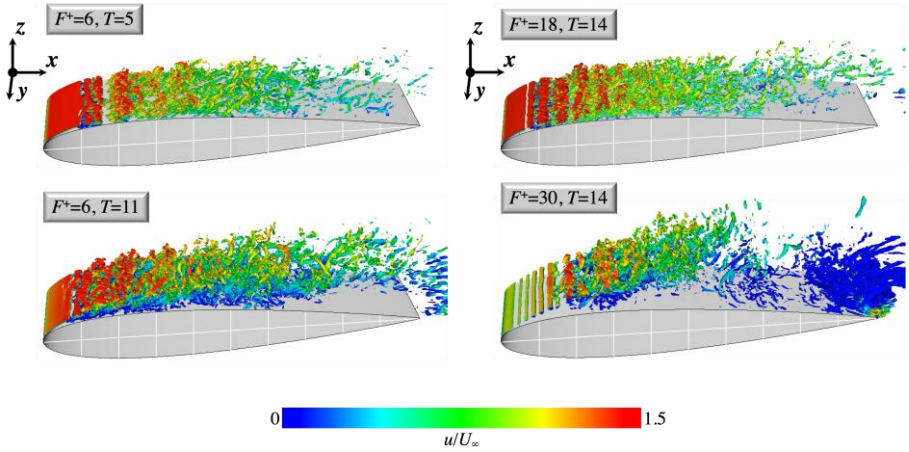

Fig. 3: Instantaneous flow fields

Publications

- Non peer-reviewed papers

T. Ogawa, K. Asada, A. Yakeno, K. Fujii, "Revisiting burst drive conditions of DBD plasma actuator for airfoil flow control", AIAA SciTech2024, Orlando, FL, U.S.A., Jan. 2024.

Usage of JSS

Computational Information

Process Parallelization Methods	MPI
Thread Parallelization Methods	Automatic Parallelization
Number of Processes	79
Elapsed Time per Case	40 Hour(s)

- **JSS3 Resources Used**

Fraction of Usage in Total Resources[*1](%): 0.01

Details

Computational Resources		
System Name	CPU Resources Used (core x hours)	Fraction of Usage[*2](%)
TOKI-SORA	358,295.52	0.02
TOKI-ST	0.00	0.00
TOKI-GP	0.00	0.00
TOKI-XM	0.00	0.00
TOKI-LM	0.00	0.00
TOKI-TST	0.00	0.00
TOKI-TGP	0.00	0.00
TOKI-TLM	0.00	0.00

File System Resources		
File System Name	Storage Assigned (GiB)	Fraction of Usage[*2] (%)
/home	40.00	0.03
/data and /data2	16,558.09	0.10
/ssd	0.00	0.00

Archiver Resources		
Archiver Name	Storage Used (TiB)	Fraction of Usage[*2] (%)
J-SPACE	0.00	0.00

[*1]: Fraction of Usage in Total Resources: Weighted average of three resource types (Computing, File System, and Archiver).

[*2]: Fraction of Usage：Percentage of usage relative to each resource used in one year.

- **ISV Software Licenses Used**

ISV Software Licenses Resources		
	ISV Software Licenses Used (Hours)	Fraction of Usage[*2] (%)
ISV Software Licenses (Total)	0.00	0.00

[*2]: Fraction of Usage：Percentage of usage relative to each resource used in one year.